INTERNATIONAL JOURNAL FOR NUMERICAL METHODS IN FLUIDS, VOL. 25, 437–454 (1997)

TRANSIENT 1D TRANSPORT EQUATION SIMULATED BY A MIXED GREEN ELEMENT FORMULATION

AKPOFURE EFEMENA TAIGBENU[1] AND OKEY OSELOKA ONYEJEKWE[2]*

[1] *Department of Civil Engineering, University of Benin, Benin City, Nigeria*
[2] *Department of Civil Engineering, University of Durban-Westville, Durban, South Africa*

SUMMARY

New discrete element equations or coefficients are derived for the transient 1D diffusion–advection or transport equation based on the Green element replication of the differential equation using linear elements. The Green element method (GEM), which solves the singular boundary integral theory (a Fredholm integral equation of the second kind) on a typical element, gives rise to a banded global coefficient matrix which is amenable to efficient matrix solvers. It is herein derived for the transient 1D transport equation with uniform and non-uniform ambient flow conditions and in which first-order decay of the containment is allowed to take place. Because the GEM implements the singular boundary integral theory within each element at a time, the integrations are carried out in exact fashion, thereby making the application of the boundary integral theory more utilitarian. This system of discrete equations, presented herein for the first time, using linear interpolating functions in the spatial dimensions shows promising stable characteristics for advection-dominant transport. Three numerical examples are used to demonstrate the capabilities of the method. The second-order-correct Crank–Nicolson scheme and the modified fully implicit scheme with a difference weighting value of two give superior solutions in all simulated examples. © 1997 by John Wiley & Sons, Ltd.

Int. J. Numer. Meth. Fluids, **25**: 437–454 (1997).

No. of Figures: 8. No. of Tables: 3. No. of References: 29.

KEY WORDS: Green element method; diffusion–advection

1. INTRODUCTION

The solution to the diffusion–advection or transport equation continues to attract considerable interest in numerical circles because of its unique features of being either a parabolic or hyperbolic equation, depending on the values of the parameters of the equation, and also because its solution process offers valuable computational experience which can be extended to the simulation of the many other flows of engineering interest. Furthermore, the areas of engineering applications where the transport equation is encountered are diverse—agriculture, water resources and environmental, chemical, petroleum engineering, etc.

Although quite a considerable number of analytic solutions exist in one and two dimensions,[1,2] their usefulness is limited to problems with simple boundary conditions and regular geometries. However, they serve one useful purpose of validating the accuracy of numerical methods. Whereas earlier numerical calculations of the transport equation were based on the finite difference method (FDM),[3,4] there has in the recent past been a shift towards the finite element approach. Standard finite

* Correspondence to: O. O. Onyejekue, Department of Civil Engineering, University of Durban-Westville, Durban, South Africa

CCC 0271–2091/97/040437–18 $17.50

Received 7 November 1995
Revised 25 September 1996

difference schemes produce for advection-dominant cases unacceptably large spurious oscillations or numerically diffused solutions.

From an earlier summary of numerical solutions of advection–diffusion by Anderson[5] and a more recent one by Zienkiewicz and Taylor[6] which focused mainly on finite-element-based schemes, it is obvious that the solution of the transport equation will continue to generate much interest in numerical circles. Finite element schemes which were based on Bobnov–Galerkin weighing functions showed similar unpleasant numerical features of spurious oscillations and a diffused or smeared front because of the difficulty encountered in the approximation of the convective term,[7] but, by adopting the upwind differencing of the advective term first observed in finite difference circles,[8] some of these unpleasant features were reduced.[9,10] A natural extension of upwind differencing in finite element applications gave rise to Petrov–Galerkin weighing functions in which the weighing function takes into account the direction of the advecting velocity vector and the relative magnitudes of diffusion and advection which are embodied in a dimensionless quantity known as the Peclet number.[11,12] The attempts seem to have heralded a flurry of activity in finite element circles. However, an evolving consensus of opinion on this large array of schemes is a return to basics and simplicity of model formulation rather than the introduction of weighting coefficients whose theoretical justification may not be quite convincing except for the fact that, under restrictive cases, better solutions are achieved.

In other circles the finite analytic method has been applied to the diffusion–advection equation.[13] Unlike in the finite difference or finite element methods, the resulting discrete algebraic equations of the governing partial differential equations are obtained from the analytic solution within each local element. A unique quality of this formulation is that both the influence of the skewed convective vector and the magnitude of convection are automatically accounted for. Onyejekwe[14] adopted a generalized co-ordinate for the one-dimensional advection–diffusion equation and, by adapting the grids to cluster around the areas of large concentration gradients, obtained fairly accurate results for high-Peclet-number flows.

Contemporary developments have been taking place in boundary element circles on accurate modelling of the transport equation. An earlier attempt by Brebbia and Skerget,[15] which employed the temporal, free space Green functions in two spatial dimensions, was applied to cases with small values of Peclet number. Another approach,[16,17] based on the fundamental solution to the 2D Laplacian operation, treated the transient problem as a quasi-steady one and offered solutions which covered the whole spectrum of Peclet number values. However, the major drawbacks of that approach were dealing with a fully populated global coefficient matrix, which greatly tasked computing resources, and the inability to accommodate medium heterogeneity. These boundary element formulations were developed for transient problems in two spatial dimensions.

It has been recognized that the boundary-only character of the boundary element theory, observed for elliptic problems and considered one of the strengths of the boundary element method (BEM), is not retained when dealing with a parabolic/hyperbolic equation like the diffusion–advection equation. Domain integration, earlier considered an undesirable numerical feature, has to be done even when the free space Green function of the constant velocity advection–dispersion operator is used.[18] However, when domain integration is implemented along the lines of the Green element approach, it is easier to handle, because the source and field nodes always remain on the same element.[19–20]

The Green's element approach, which derives a system of discrete element equations based on the singular integral boundary element concept, has the advantages of producing a sparse banded global coefficient matrix which is easier to invert and of readily accommodating medium heterogeneity. The demonstration of the method in handling non-linear problems eliminates one of the earlier assertions that the boundary element theory is inapplicable to non-linear problems.[21–25]

In effect, what we have achieved is to enhance the range of applicability of the boundary integral theory, but not to claim the superiority of the GEM over other traditional methods. Underpinning this objective is our belief that there should be a co-operation of numerical methods whereby the strengths of any method are exploited and adapted for use. With this in mind we combined the elegant boundary integral representation of the governing differential equation with the versatile domain discretization approach of the FEM to formulate a technique known as the GEM.

Here the Green element equations are derived for the 1D transient diffusion–advection equation with first-order decay under uniform and non-uniform ambient flow situations using the free space Green function of the diffusive term. The new discrete element equations or coefficients obtained exhibit stable characteristics even for large Peclet number values. Three numerical examples for which analytic solutions are available are used to demonstrate the capability of the method.

2. THE GREEN ELEMENT FORMULATION

The partial differential equation that describes one-dimensional transport with first-order decay in a homogeneous medium under transient fluid flow conditions is given by

$$D\frac{\partial^2 c(x,t)}{\partial x^2} - u(x,t)\frac{\partial c(x,t)}{\partial x} - \frac{\partial c(x,t)}{\partial t} - \mu c = 0 \quad \text{on } x_0 \leqslant x \leqslant x_L, \tag{1}$$

in which $c = c(x,t)$ is the solution concentration, D is the hydrodynamic dispersion coefficient ($\mathrm{L}^2\ \mathrm{T}^{-1}$), $u = u(x,t)$ is the velocity in the x-direction ($\mathrm{L}\,\mathrm{T}^{-1}$), x and t are the spatial and temporal independent variables respectively. μ is the rate constant of first-order decay for a non-conservative pollutant (T^{-1}) and $L = x_0 - x_L$ is the length of the flow domain. Equation (1) continues to receive enormous interest because of its extensive applications in the areas of agriculture, chemical environmental and water resources engineering. The solution of (1) requires information on the boundary conditions at x_0 and x_L and data on $c(x,t)$ at the initial time t_0. The first-type or Dirichlet condition specifies the concentration at the end points:

$$c(x_0,t) = g_0(t), \qquad c(x_L,t) = t_L(t). \tag{2a}$$

The second-type or flux-type or Neumann condition specifies the flux of the substance being transported:

$$D\frac{\partial c(x_0,t)}{\partial x} = f_0(t), \qquad D\frac{\partial c(x_L,t)}{\partial x} = f_L(t). \tag{2b}$$

Alternatively, an appropriate combination of the two may be used. The initial data specify the concentration at the initial time t_0:

$$c(x,t_0) = c_0(x), \quad x_0 \leqslant x \leqslant x_L. \tag{2c}$$

Our current Green element formulation is based on the Fredholm singular integral theory which employs the free space Green function of the term with the highest derivative, namely $\partial^2/\partial x^2$. We propose a differential equation complementary to (1) of the form

$$\frac{\mathrm{d}^2 G}{\mathrm{d}x^2} = \delta(x - x_i), \quad -\infty \leqslant x \leqslant \infty, \tag{3}$$

in which $\delta(x - x_i)$ is the Dirac delta function and x_i is commonly referred to as the source point. The general expression of the solution to (3) is of the form

$$G(x,x_i) = \tfrac{1}{2}(|x - x_i| + k), \tag{4}$$

where k is an arbitrary constant. (Although k is an arbitrary constant, its value has to be judiciously chosen, otherwise some of the diagonal elements could have zero value. Certainly the value of$k$ cannot be set to zero in our formulation because this leads to the diagonal element entry for the flux in the global coefficient matrix being zero, thereby producing a singular matrix.) We elect to set k to unity. $G(x, x_i)$ is referred to as the free space Green function or the fundamental solution or the unit response function. It is the response of a system governed by (3) due to an instantaneous unit input. Green's second identity is employed in transforming the differential equation into an integral one. It is stated for two functions $G(x, x_i)$ and $c(x, t)$ which should be at least twice differentiable with respect to the spatial variable x:

$$\int_{x_0}^{x_L} \left(c\frac{\mathrm{d}^2 G}{\mathrm{d}x^2} - G\frac{\partial^2 c}{\partial x^2} \right) \mathrm{d}x = \left[c\frac{\mathrm{d}G}{\mathrm{d}x} - G\frac{\partial c}{\partial x} \right]_{x=x_0}^{x=x_L}. \tag{5}$$

Introducing equations (1) and (3) into (5) yields

$$D\left(-\lambda_i c(x_i, t) + \left[c\frac{\partial G}{\partial x} \right]_{x=x_0}^{x=x_L} - \left[G\frac{\partial c}{\partial x} \right]_{x=x_0}^{x=x_L} \right) + \int_{x_0}^{x_L} G\left(u\frac{\partial c}{\partial x} + \frac{\partial c}{\partial t} + \mu c \right) \mathrm{d}x = 0, \tag{6}$$

in which

$$\lambda_i = \int_{-\infty}^{x_i} \delta(x - x_i)\mathrm{d}x + \int_{x_i}^{\infty} \delta(x - x_i)\mathrm{d}x = \int_{x_i-\varepsilon}^{x_i} \delta(x - x_i)\mathrm{d}x + \int_{x_i}^{x_i+\varepsilon} \delta(x - x_i)\mathrm{d}x, \tag{7}$$

where ε is any small positive quantity. Using the property of the Dirac delta function γ_i takes the value of unity if x_i is within the interval $x_0 < x < x_L$ and $\lambda_i = 0{\cdot}5$ if x_i is at the end points of the flow length. The derivative of the free space Green function with respect to x is given by the expression

$$\frac{\mathrm{d}G(x, x_i)}{\mathrm{d}x} = \tfrac{1}{2}[H(x - x_i) - H(x_i - x)], \tag{8}$$

where H is the Heaviside function defined as

$$H(x - x_i) = \begin{cases} 1, & x > x_i, \\ 0, & x < x_i. \end{cases} \tag{9}$$

The flow region is discretized into M line segments with a typical segment of element (e) denoted by the interval $[x_1^{(e)}, x_2^{(e)}]$ (see Figure 1). The discretized form of the integral equation (6) when the flow region is discretized is given by

$$\sum_{e=1}^{M} D\left(-\lambda_i^{(e)} c^{(e)}(x_i, t) + \left[c\frac{\partial G}{\partial x} \right]_{x=x_i^{(e)}}^{x=x_2^{(e)}} - \left[G\frac{\partial c}{\partial x} \right]_{x=x_1^{(e)}}^{x=x_2^{(e)}} \right) + \int_{x_1^{(e)}}^{x_2^{(e)}} G\left(u\frac{\partial c}{\partial x} + \frac{\partial c}{\partial t} + \mu c \right) \mathrm{d}x = 0. \tag{10}$$

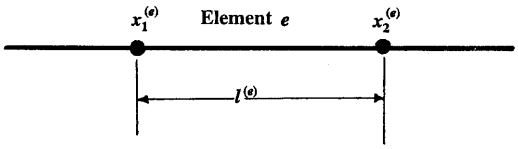

Figure 1. Definition sketch for linear 1D element

To evaluate the line integral over a typical element, it is necessary to prescribe a distribution of c, u and $\partial c/\partial x$ over each element. We elect to use one of the simplest interpolation functions—a linear one—to approximate these quantities:

$$c(x,t) = \Omega_1^{(e)} c_1^{(e)}(t) + \Omega_2^{(e)} c_2^{(e)}(t), \quad \phi(x,t) = \Omega_1^{(e)} \phi_1^{(e)}(t) + \Omega_2^{(e)} \phi_2^{(e)}(t), \quad u(x,t) = \Omega_1^{(e)} u_1^{(e)}(t) + \Omega_2^{(e)} u_2^{(e)}(t), \tag{11}$$

in which $\phi = \partial c/\partial x$, the quantity $c_1^{(e)}(t)$, for instance, denotes the value of $c(x,t)$ at $x_1^{(e)}$ at time t and the element interpolating functions $\Omega_1^{(e)}$ and $\Omega_1^{(e)}$ are given by

$$\Omega_1^{(e)}(\zeta) = 1 - \zeta, \qquad \Omega_2^{(e)}(\zeta) = \zeta, \tag{12}$$

where $\zeta = (x - x_1^{(e)})/l^{(e)}$, $0 \leqslant \zeta \leqslant 1$, is a local co-ordinate that has its origin at $x_1^{(e)}$ and $l^{(e)}$ is the length of the element. The local co-ordinate ζ is a more appropriate one in Green element calculations because it greatly simplifies the evaluation of the line integrals. Introducing equations (4), (8) and (11) into (10) yields

$$\begin{aligned}
&\sum_{e=1}^{M} D\{-2\lambda_i^{(e)} c_i^{(e)} + [H(x_2^{(e)} - x_i^{(e)}) - H(x_i^{(e)} - x_2^{(e)})]c_2^{(e)} - [H(x_1^{(e)} - x_i^{(e)}) - H_i^{(e)} - x_1^{(e)})]c_1^{(e)} \\
&\quad - (|x_2^{(e)} - x_i^{(e)}| + 1)\phi_2^{(e)} + (|x_1^{(e)} - x_i^{(e)}| + 1)\phi_1^{(e)}\} \\
&\quad + \int_{x_1^{(e)}}^{x_2^{(e)}} (|x - x_i^{(e)}| + 1)\left[(\Omega_1^{(e)} u_1^{(e)} + \Omega_2^{(e)} u_2^{(e)})(\Omega_1^{(e)} \phi_1^{(e)} + \Omega_2^{(e)} \phi_2^{(e)}) + \Omega_1^{(e)}\left(\frac{\mathrm{d}c_1^{(e)}}{\mathrm{d}t} + \mu c_1^{(e)}\right)\right. \\
&\quad \left. + \Omega_2^{(e)}\left(\frac{\mathrm{d}c_2^{(e)}}{\mathrm{d}t} + \mu c_2^{(e)}\right)\right]\mathrm{d}x = 0.
\end{aligned} \tag{13}$$

Two sets of discretized equations are obtained from (13): the first comes from considering the source node $x_i^{(e)}$ located at $x_1^{(e)}$, giving

$$\begin{aligned}
&\sum_{e=1}^{M} D[-c_1^{(e)} + c_2^{(e)} + \phi_1^{(e)} - (1 + l^{(e)})\phi_2^{(e)}] \\
&\quad + l^{(e)} \int_0^1 (1 + l^{(e)}\zeta)\left[(\Omega_1^{(e)} u_1^{(e)} + \Omega_2^{(e)} u_2^{(e)})(\Omega_1^{(e)} \phi_1^{(e)} + \Omega_2^{(e)} \phi_2^{e}) + \Omega_1^{(e)}\left(\frac{\mathrm{d}c_1^{(e)}}{\mathrm{d}t} + \mu c_1^{(e)}\right)\right. \\
&\quad \left. + \Omega_2^{(e)}\left(\frac{\mathrm{d}u_2^{(e)}}{\mathrm{d}t} + \mu c_2^{(e)}\right)\right]\mathrm{d}\zeta = 0,
\end{aligned} \tag{14a}$$

and the second comes from considering the source node $x_i^{(e)}$ located at $x_2^{(e)}$, giving

$$\begin{aligned}
&\sum_{e=1}^{M} D[c_1^{(e)} - c_2^{(e)} + (1 + l^{(e)})\phi_1^{(e)} - \phi_2^{(e)}] \\
&\quad + l^{(e)} \int_0^1 [1 + l^{(e)}(1 - \zeta)]\left[(\Omega_1^{(e)} u_1^{(e)} + \Omega_2^{(e)} u_2^{(e)})(\Omega_1^{(e)} \phi_1^{(e)} + \Omega_2^{(e)} \phi_2^{(e)}) + \Omega_1^{(e)}\left(\frac{\mathrm{d}c_1^{(e)}}{\mathrm{d}t} + \mu c_1^{(e)}\right)\right. \\
&\quad \left. + \Omega_2^{(e)}\left(\frac{\mathrm{d}u_2^{(e)}}{\mathrm{d}t} + \mu c_2^{(e)}\right)\right]\mathrm{d}\zeta = 0.
\end{aligned} \tag{14b}$$

Combination of (14a,b) into matrix form yields

$$\sum_{e=1}^{M} DR_{ij}^{(e)} c_j^{(e)} + (DL_{ij}^{(e)} + V_{ikj}^{(e)} u_k^{(e)})\phi_j^{(e)} + T_{ij}^{(e)} \left(\frac{\mathrm{d}u_j^{(e)}}{\mathrm{d}t} + \mu c_j^{(e)} \right) = 0, \quad i, j, k = 1, 2, \tag{15}$$

in which the elemental matrices are

$$R_{ij}^{(e)} = \begin{bmatrix} -1 & 1 \\ 1 & -1 \end{bmatrix} = (-1)^{(i+j-1)}, \quad i, j = 1, 2, \tag{16a}$$

$$L_{ij}^{(e)} = \begin{bmatrix} 1 & -(1 + l^{(e)}) \\ 1 + l^{(e)} & -1 \end{bmatrix}, \quad i, j = 1, 2, \tag{16b}$$

$$\begin{aligned} T_{11}^{(e)} &= l^{(e)} \int_0^1 (1 - \zeta)(1 + l^{(e)}\zeta)\mathrm{d}\zeta = T_{22}^{(e)} = l^{(e)} \int_0^1 \zeta[1 + l^{(e)}(\zeta - 1)]\mathrm{d}\zeta = \frac{l^{(e)}(3 + l^{(e)})}{6}, \\ T_{12}^{(e)} &= l^{(e)} \int_0^1 \zeta(1 + l^{(e)}\zeta)\mathrm{d}\zeta = T_{21} = l^{(e)} \int_0^1 (1 - \zeta)[1 + l^{(e)}(\zeta - 1)]\mathrm{d}\zeta = \frac{1^{(e)}(3 + 2l^{(e)})}{6}, \end{aligned} \tag{16c}$$

$$\begin{aligned} V_{111}^{(e)} &= l^{(e)} \int_0^1 (1 - \zeta)^2(1 + l^{(e)}\zeta)\mathrm{d}\zeta = V_{222}^{(e)} = l^{(e)} \int_0^1 \zeta^2[1 + l^{(e)}(\zeta - 1)]\mathrm{d}\zeta = \frac{l^{(e)}(4 + l^{(e)})}{12}, \\ V_{112}^{(e)} &= V_{121}^{(e)} = l^{(e)} \int_0^1 \zeta(1 - \zeta)(1 + l^{(e)}\zeta)\mathrm{d}\zeta = V_{212}^{(e)} = V_{221}^{(e)} = l^{(e)} \int_0^1 \zeta(1 - \zeta)[1 + l^{(e)}(\zeta - 1)]\mathrm{d}\zeta \\ &= \frac{l^{(e)}(2 + l^{(e)})}{12}, \\ V_{122}^{(e)} &= l^{(e)} \int_0^1 \zeta^2(1 + l^{(e)}\zeta)\mathrm{d}\zeta = V_{211}^{(e)} = l^{(e)} \int_0^1 (1 - \zeta)^2[1 + l^{(e)}(\zeta - 1)]\mathrm{d}\zeta = \frac{l^{(e)}(4 + 3l^{(e)})}{12}. \end{aligned} \tag{16d}$$

Equation (15) is referred to as the system of element equations of the Green element formulation of the diffusion–advection equation under non-uniform flow. It provides all the information required to solve for the nodal unknowns. Because there are two degrees of freedom at each node, i.e. c and ϕ, the formulation can be said to be a mixed formulation. The advantage of such a mixed formulation is that the primary variable c and its spatial derivative ϕ are approximated by the same interpolation basis functions, ensuring that their accuracies are of the same order. For our current formulation where we have employed linear basis interpolation functions to approximate c and ϕ within the element, this means that those quantities will be continuous at the nodes, i.e. have C^0 continuity. This approach is in contrast with those of other numerical methods where ϕ is treated as a secondary variable that is obtained from the primary variable by numerical differentiation, thereby reducing by one order the accuracy of the spatial derivative of the primary variable. Equation (15) is a system of first-order linear differential equations in time which can be solved for c and ϕ at the nodes by employing an appropriate approximation of the temporal derivative. We elect to use the two-level

time discretization scheme that approximates the temporal derivative at $t = t_{m+\alpha} = t_m + \alpha\Delta t$ by a difference expression so that equation (15) becomes

$$\sum_{e=1}^{M} \alpha[DR_{ij}^{(e)} c_{j,m+1}^{(e)} + (DL_{ij}^{(e)} + V_{ijk}^{(e)} u_{k,m+1}^{(e)})\phi_{j,m+1}^{(e)}] + (1-\alpha)[DR_{ij}^{(e)} c_{j,m}^{(e)} + (DL_{ij}^{(e)} + V_{ijk}^{(e)} u_{k,m}^{(e)})\phi_{j,m}^{(e)}]$$
$$+ T_{ij}^{(e)}\left(\frac{1}{\Delta t}(c_{j,m+1}^{(e)} - c_{j,m}^{(e)}) + \mu[\alpha c_{j,m+1}^{(e)} + (1-\alpha)c_{j,m}^{(e)}]\right) = 0, \quad i,j,k = 1,2, \quad 0 \leqslant \alpha \leqslant 1, \tag{17}$$

in which α is a time weighting factor, the subscripts $m+1$ and m denote the current and previous time levels respectively and $\Delta t = t_{m+1} - t_m$ is the time step.

When the velocity of the transporting fluid is uniform, i.e. $U(t) = U(x,t)$, then it is no longer necessary to express the velocity as a linear function of its nodal values. In that case the integral equation given by (13) becomes

$$\sum_{e=1}^{M} D\{-2\lambda_i^{(e)} c_i^{(e)} + [H(x_2^{(e)} - x_i^{(e)}) - H(x_i^{(e)} - x_2^{(e)})]c_2^{(e)} - [H(x_1^{(e)} - x_1^{(e)}) - H(x_i^{(e)} - x_i^{(e)})]c_1^{(e)}$$
$$- (|x_2^{(e)} - x_i^{(e)}| + 1)\phi_2^{(e)} + (|x_1^{(e)} - x_i^{(e)}| + 1)\phi_1^{(e)}\}$$
$$+ \int_{x_1^{(e)}}^{x_2^{(e)}} (|x - x_i^{(e)}| + 1)\left[\Omega_1^{(e)}\left(U\phi_1^{(e)} + \frac{\mathrm{d}c_1^{(e)}}{dt} + \mu c_1^{(e)}\right) + \Omega_2^{(e)}\left(U\phi_2^{(e)} + \frac{\mathrm{d}c_2^{(e)}}{(e)dt} + \mu c_2^{(e)}\right)\right]\mathrm{d}x. \tag{18}$$

Employing the generalized two-level time scheme, the above equation gives a system of discrete equations of the form

$$\sum_{e=1}^{M} \alpha[DR_{ij}^{(e)} c_{j,m+1}^{(e)} + (DL_{ij}^{(e)} + U_{m+1} T_{ij}^{(e)})\phi_{j,m+1}^{(e)}] + (1-\alpha)[DR_{ij}^{(e)} c_{j,m}^{(e)} + (DL_{ij}^{(e)} + U_m T_{ij}^{(e)})\phi_{j,m}^{(e)}]$$
$$+ T_{ij}^{(e)}\left(\frac{1}{\Delta t}(c_{j,m+1}^{(e)} - c_{j,m}^{(e)}) + \mu[\alpha c_{j,m+1}^{(e)} + (1-\alpha)c_{j,m}^{(e)}]\right) = 0, \quad i,j,k = 1,2, \quad 0 \leqslant \alpha \leqslant 1. \tag{19}$$

Equation (19) is a system of discrete equations for the transient 1D diffusion–advection equation under uniform flow. In view of another version of this equation that will shortly be derived, we shall refer to this model as the first quasi-steady Green element model for the diffusion–advection equation under uniform flow or GEDAU-1 model. Another model of (19) can be derived for the uniform velocity case by recognizing that the integral over a typical element for the advection term in (10) can be transformed in the following manner:

$$\int_{x_1^{(e)}}^{x_2^{(e)}} UG\frac{\partial C}{\partial x}\mathrm{d}x = U\int_{x_1^{(e)}}^{x_2^{(e)}} \left(\frac{\partial(cG)}{\partial x} - c\frac{\mathrm{d}G}{\mathrm{d}x}\right)\mathrm{d}x = U\left(cG\Big|_{x_1^{(e)}}^{x_2^{(e)}} - \int_{x_1^{(e)}}^{x_2^{(e)}} c\frac{\mathrm{d}G}{\mathrm{d}x}\mathrm{d}x\right). \tag{20}$$

It can now be verified that with the above transformation and the introduction of the expressions for G and $\mathrm{d}G/\mathrm{d}x$ and the linear interpolation distribution for c the advective term with uniform flow becomes

$$2\int_{x_1^{(e)}}^{x_2^{(e)}} UG\frac{\partial c}{\partial x}\mathrm{d}x = \frac{U}{2}\left(\begin{bmatrix} -1 & 1+l^{(e)} \\ -(1+l^{(e)}) & 1 \end{bmatrix} - l^{(e)}\begin{bmatrix} \int_0^1 (1-\zeta)\mathrm{d}\zeta & \int_0^1 \zeta\mathrm{d}\zeta \\ -\int_0^1 (1-\zeta)\mathrm{d}\zeta & -\int_0^1 \zeta\mathrm{d}\zeta \end{bmatrix}\right)\begin{pmatrix} c_1^{(e)} \\ c_2^{(e)} \end{pmatrix}$$

$$= UP_{ij}^{(e)}c_j^{(e)} = \frac{U}{2}\begin{bmatrix} -(2+l^{(e)}) & 2+l^{(e)} \\ -(2+l^{(e)}) & 2+l^{(e)} \end{bmatrix}\begin{pmatrix} c_1^{(e)} \\ c_2^{(e)} \end{pmatrix}, \quad i,j=1,2. \tag{21}$$

With this treatment given to the advection term, the system of discrete element equations incorporating the generalized two-level time discretization schemes becomes

$$\sum_{e=1}^{M} \alpha[D(R_{ij}+U_{m+1}P_{ij}^{(e)})^{(e)}c_{j,m+1}^{(e)} + DL_{ij}^{(e)}\phi_{j,m+1}^{(e)}] + (1-\alpha)[(DR_{ij}^{(e)}+U_mP_{ij}^{(e)})c_{j,m}^{(e)} + DL_{ij}^{(e)}\phi u_{j,m}^{(e)}]$$
$$+ T_{ij}^{(e)}\left(\frac{1}{\Delta t}(c_{j,m+1}^{(e)} - c_{j,m}^{(e)}) + \mu[\alpha c_{j,m+1}^{(e)} + (1-\alpha)c_{j,m}^{(e)}]\right) = 0, \quad i,j,k=1,2, \quad 0 \leqslant \alpha \leqslant 1. \tag{22}$$

We shall refer to this model as the second quasi-steady uniform flow advection–diffusion Green element model (GEDAU-2 model). Another approximation of the temporal derivative could also be incorporated into the Green element model. It comes from the use of a modified fully implicit scheme that approximates the temporal derivative as

$$\left.\frac{\mathrm{d}c_j^{(e)}}{\mathrm{d}t}\right|_{t=t_{m+1}} = \frac{\mathrm{d}c_{j,m+1}^{(e)}}{\mathrm{d}t} \approx \frac{\alpha}{\Delta t}(c_{j,m+1}^{(e)} - c_{j,m}^{(e)}) + (1-\alpha)\frac{\mathrm{d}c_{j,m}^{(e)}}{\mathrm{d}t}, \quad 1 \leqslant \alpha \leqslant 2. \tag{23}$$

With (23) we present, without any explanation, other versions of the discrete equations (17), (19) and (22) when the modified fully implicit scheme is incorporated.

Using the modified fully implicit scheme, equation (17) becomes

$$\sum_{e=1}^{M} [DR_{ij}^{(e)}c_{j,m+1}^{(e)} + (DL_{ij}^{(e)} + V_{ijk}^{(e)}u_{k,m+1}^{(e)}\phi_{j,m+1}^{(e)})] + T_{ij}^{(e)}\left(\frac{\alpha}{\Delta t}(c_{j,m+1}^{(e)} - c_{j,m}^{(e)}) + (1-\alpha)\frac{\mathrm{d}c_{j,m}^{(e)}}{\mathrm{d}t} + \mu c_{j,m+1}^{(e)}\right)$$
$$= 0, \quad i,j,k=2, \quad 1 \leqslant \alpha \leqslant 2, \tag{24}$$

equation (19) becomes

$$\sum_{e=1}^{M} [DR_{ij}^{(e)}c_{j,m+1}^{(e)} + (DL_{ij}^{(e)} + U_{m+1}T_{ij}^{(e)})\phi_{j,m+1}^{(e)}] + T_{ij}^{(e)}\left(\frac{\alpha}{\Delta t}(c_{j,m+1}^{(e)} - c_{j,m}^{(e)}) + (1-\alpha)\frac{\mathrm{d}c_{j,m}^{(e)}}{\mathrm{d}t} + \mu c_{j,m+1}^{(e)}\right)$$
$$= 0, \quad i,j,k=1,2, \quad 1 \leqslant \alpha \leqslant 2, \tag{25}$$

and equation (22) becomes

$$\sum_{e=1}^{M} (DR_{ij}^{(e)} + U_{m+1}P_{ij})c_{j,m+1}^{(e)} + DL_{ij}^{(e)}\phi_{j,m+1}^{(e)} + T_{ij}^{(e)}\left(\frac{\alpha}{\Delta t}(c_{j,m+1}^{(e)} - c_{j,m}^{(e)}) + (1-\alpha)\frac{\mathrm{d}c_{j,m}^{(e)}}{\mathrm{d}t} + \mu c_{j,m+1}^{(e)}\right)$$
$$= 0, \quad i,j,k=1,2, \quad 1 \leqslant \alpha \leqslant 2. \tag{26}$$

It now remains to assemble the elemental matrices for all M elements, which should be done so that two degrees of freedom are maintained at each node. At this stage as well the boundary and initial conditions should be effected. The resultant global equation is given by

$$A_{ij}\begin{pmatrix} c_j \\ \phi_j \end{pmatrix} = S_i. \tag{27}$$

The global coefficient matrix is banded with a half-bandwidth of two and with a row dimension that is twice the number of elements. The matrix can be solved quite efficiently with a banded matrix solver for the nodal quantities c and ϕ at the current time $t_{m+1} = t_m + \Delta t$.

3. NUMERICAL EXPERIMENTS AND DISCUSSION

Three numerical examples of transient 1D diffusion–advection problems are used to demonstrate the capabilities and characteristics of the numerical method. The first is the classical 1D transport problem which is used quite often to assess the performance of many numerical schemes. The problem is governed by (1) with $\mu = 0$ and the contaminant is transported under uniform velocity conditions. The boundary and initial conditions are

$$c(0, t) = 1, \qquad \frac{\partial c(x = \infty, t)}{\partial x} = 0, \qquad c(x, t = 0) = 0. \tag{28}$$

The solution to this transport problem with the above conditions is well known[26] and so is not repeated here. To assess the performance of the numerical scheme in simulating this example, two cases or modes of transport processes are examined. One case is a marginally advection–dominant transport process represented by a local Peclet number $Pe = 2$ ($Pe = Ul/D$, where l is the spatial size of each element) and the second case represents a transport process of strong advection dominance with a local Peclet number $Pe = 50$. The numerical calculations are carried out with a uniform ambient velocity $U = 1$ and spatial size of each element $l = 0{\cdot}025$ and the solution of the concentration front is presented at $t = 0{\cdot}5$. The influence of temporal discretization on the quality of the numerical solutions is measured by the dimensionless parameter known as the Courant number, which is expressed as $Cr = U\Delta t/l$, and the two values of Courant number are employed in the calculations: $Cr = 0{\cdot}2$ and 1. A small value of Courant number represents a numerical computation with small time steps. A number of numerical experiments are carried out using this example with the aim of examining the quality of the numerical solutions obtained by incorporating the various time discretization schemes into the Green element model for uniform flow conditions (GEDAU-1). Figure 2(a) and 2(b) show plots of the analytical and numerical solutions for the marginally advection–dominant transport case ($Pe = 2$) with Courant numbers $Cr = 0{\cdot}2$ and 1 respectively. Although four values of time weighting factor of the generalized two-level time discretization scheme of (19) ($\alpha = 0{\cdot}5$, 0·67, 0·75 and 1) and four values of time weighting factor of the modified implicit scheme of (26) ($\alpha = 1{\cdot}25$, 1·5, 1·75 and 2) were used in the numerical calculations for this marginally advection–dominant transport mode, only results using one of the weighting values are presented because of the cluster of solutions. However, the quality of the solutions using these eight values of time discretization parameter is best assessed from Table I, which gives the l_2 error norm e_l, the peak concentration error e_p (indicative of the overshoot) and the maximum negative concentration

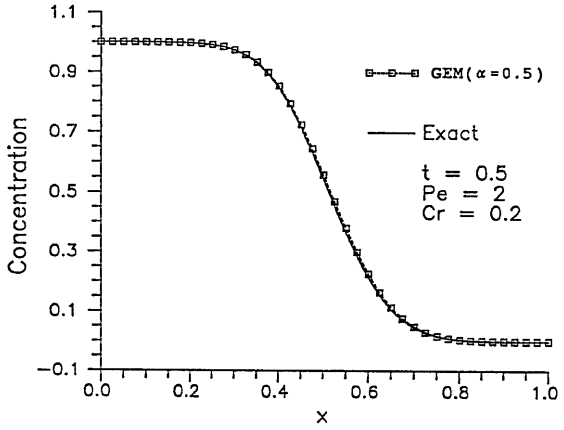

Figure 2(a). GEM and exact solution, of example 1 for $Pe = 2$ and $Cr = 0{\cdot}2$

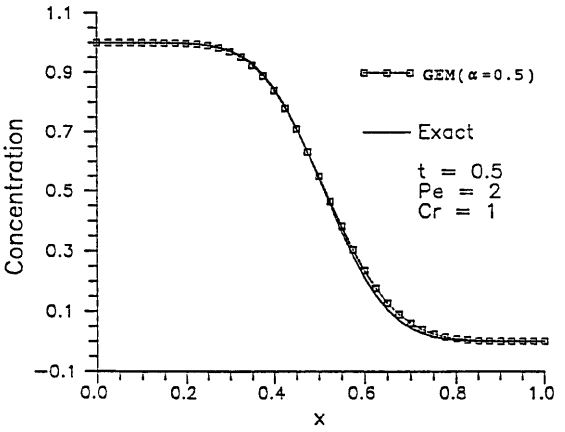

Figure 2(b). GEM and exact solutions of example 1 for $Pe = 2$ and $Cr = 1$

Table I. Accuracy assessment values of numerical solutions with various time discretization schemes for example 1 ($Pe = 2$)

	$Cr = 0{\cdot}2$			$Cr = 1$		
α	e_l ($\times 10^{-2}$)	e_p ($\times 10^{-5}$)	e_n	e_l ($\times 10^{-2}$)	e_p ($\times 10^{-5}$)	e_n
0·5	4·29	0·0	0·0	3·53	0·20	0·0
0·67	4·95	9·54	0·0	12·30	0·0	0·0
0·75	5·70	0·0	0·0	17·34	9·54	0·0
1	8·57	0·0	0·0	30·36	0·0	0·0
1·25	6·24	0·0	0·0	20·73	0·0	0·0
1·5	4·96	0·0	0·0	13·31	0·0	0·0
1·75	4·39	0·0	0·0	7·51	0·0	0·0
2	4·29	0·0	0·0	3·80	0·0	0·0

error e_n. (The last parameters are, for this example, indicative of spurious oscillations or wiggles.) The expressions of these three error estimates are

$$e_l = \left(\sum_i [c_i^N(t) - c_i^E]^2 \right)^{0.5}, \qquad e_p = |\max c_i^N(t) - \max c_i^E(t)|, \qquad e_n = \max |c_i^N(t) < 0|, \tag{29}$$

where the superscripts N and E represent the numerical and exact solutions respectively and the subscript i indicates the spatial nodal locations where the concentration values are computed. The results in Table I show that the numerical calculations with time discretization weighting values $\alpha = 0{\cdot}5$ and 2 produce the best solutions and for a local Peclet number $Pe = 2$ the numerical results using Courant numbers $Cr = 0{\cdot}2$ and 1 do not differ appreciably. For the strongly advection-dominant transport case with $Pe = 50$ the exact and numerical solutions with the eight values of time discretization parameter are presented in Figures 3(a) and 3(b) for $Cr = 0{\cdot}2$ and in Figures 3(c) and 3(d) for $Cr = 1$. Table II gives the values of accuracy parameters for the various time discretization schemes and $Cr = 0{\cdot}2$ and 1. The results for this advection-dominant transport show that the quality of the numerical solution is highly dependent on the value of Courant number or size of time step used in the computations as well as the time discretization scheme employed. For all practical purposes the numerical solutions are free of wiggles or spurious oscillations at the downstream end of the concentration front; the scheme with $\alpha = 2$ gave the best approximation of the sharp front, although it has significant oscillations upstream of the front. The temporal discretization scheme with difference weighting value $\alpha = 1$ (fully implicit scheme) gave the most diffused or dissipative solution, although it was completely free from oscillations upstream and downstream of the concentration front even for $Cr = 1$. These results indicate that for advection–dominant transport, small values of Courant number or small time steps have to be incorporated in the calculations to achieve reasonably good results when linear interpolation functions are used to approximate the dependent variables in the spatial dimension. Also incorporating the fully modified time discretization with weight $\alpha = 2$ into the Green element model offers some advantage in the quality of numerical solution.

Since this classical example of transport occurs under uniform ambient velocity, we used the more challenging case of advection-dominant transport to assess the performance of the two models (GEDAU-1 and GEDAU-2) given by (19) and (22). Without carrying out any numerical calculations

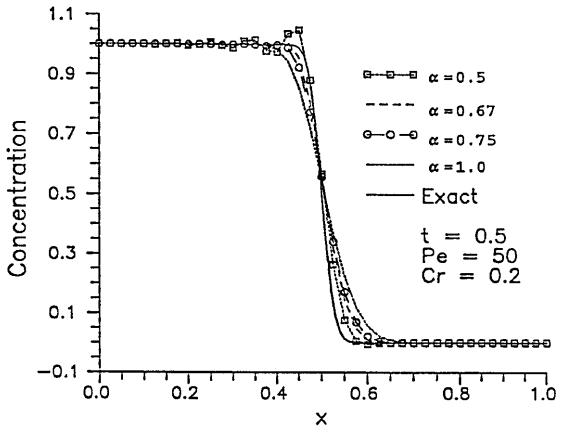

Figure 3(a). Performance of two-level time discretization schemes on example 1 for $Pe = 50$ and $Cr = 0{\cdot}2$

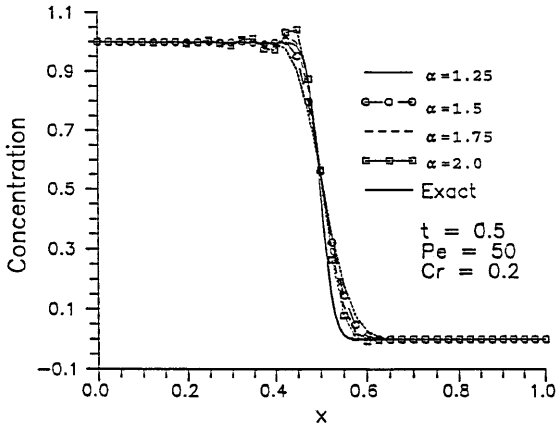

Figure 3(b). Performance of modified fully implicit time discretization schemes on example 1 for $Pe = 50$ and $Cr = 0{\cdot}2$

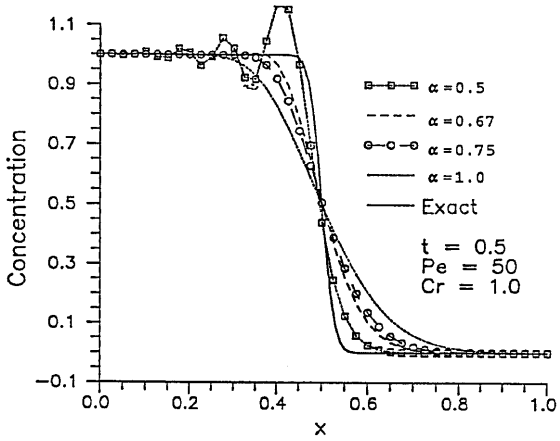

Figure 3(c). Performance of two-level discretization schemes on example 1 for $Pe = 50$ and $Cr = 1$

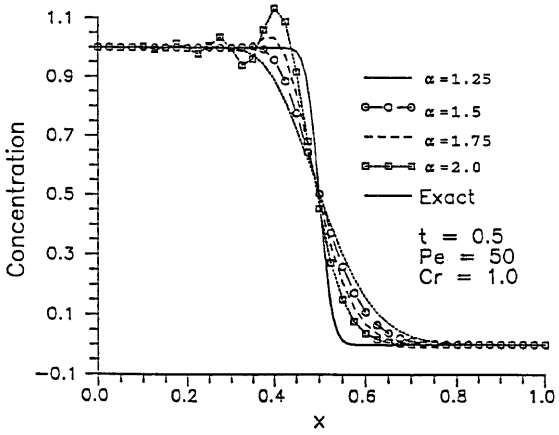

Figure 3(d). Performance of modified fully implicit time discretization schemes on example 1 for $Pe = 50$ and $Cr = 1$

Table II. Accuracy assessment values of numerical solutions with various time discretization schemes for example 1 ($Pe = 50$)

	$Cr = 0{\cdot}2$			$Cr = 1$		
α	e_l ($\times 10^{-1}$)	e_p ($\times 10^{-3}$)	e_n ($\times 10^{-3}$)	e_l ($\times 10^{-1}$)	e_p ($\times 10^{-3}$)	e_n
0·5	1·81	47·55	5·44	3·70	173·2	0·0
0·67	2·57	5·76	0·58	5·05	5·04	0·0
0·75	3·01	1·35	0·16	6·00	0·15	0·0
1	4·07	0·52	0·0	7·91	0·015	0·0
1·25	3·25	0·96	0·06	6·55	0·044	0·0
1·5	2·59	0·046	0·56	5·26	3·99	0·0
1·75	2·09	23·80	1·97	4·04	34·11	0·0
2	1·81	44·08	5·10	3·54	134·7	0·0

on this example, we can highlight the similarities and dissimilarities of the two models. Theoretically both models are the same: the transformation of (2) does not introduce any approximation to the formulation. However, to achieve the system of discrete equations, the distribution of the dependent variables is approximated by some interpolating functions, which is where the two models differ. While the first model approximates the first derivative of $c(x, t)$, i.e. $\phi(x, t)$, of the advective term by linear interpolation functions, the second model approximates the concentration $c(x, t)$ by the same set of interpolating functions. Thus the difference between the two formulations will depend on which of them gives a better approximation of those quantities in the advection term. To determine the one which gives a better approximation of the advection term, we compare the exact solutions for $c(x, t = 0{\cdot}5)$ and $[\partial c(x, t = 0{\cdot}5)/\partial x]l$ or $\phi(x, t = 0{\cdot}5)l$ and their linear interpolation profiles in Figures 4(a) and 4(b) for the case with $Pe = 50$. (Note that we have intentionally made the vertical scales of the two plots the same for ease of comparison.) These two figures show that there is, for this example, no obvious advantage in using either of the models. Actual calculations were carried out on this example using both model and their solutions were virtually the same. The only instance when one model will give a better result is when a linear approximation fits either the distribution of $c(x, t)$ or the product of the spatial size and the distribution of $\phi(x, t)$ better than the other.

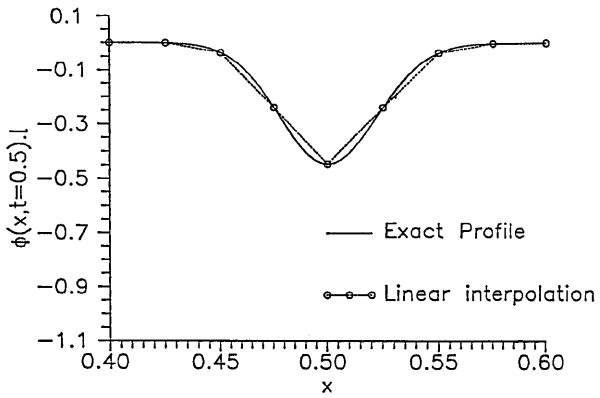

Figure 4(a). Effect of linear interpolation of derivative of concentration profile by GEDAU-1 model approximation of advective term using example 1 with $Pe = 50$

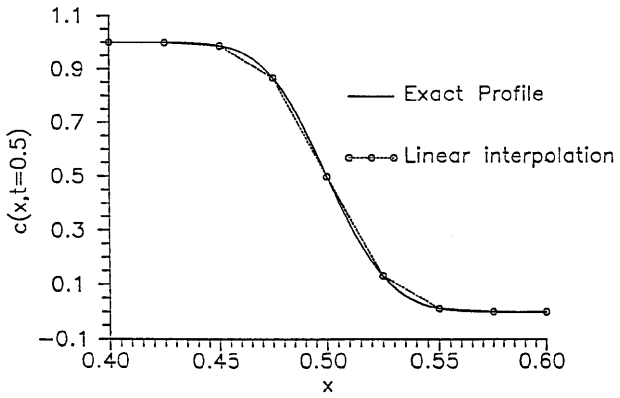

Figure 4(b). Effect of linear interpolation of concentration profile by GEDAU-2 model approximation of advective term using example 1 with $Pe = 50$

Our second example is one in which an initial Gauss-hill concentration profile is subjected to hydrodynamic dispersion and advection. The boundary conditions and initial Gauss-hill profile are given by

$$c(x = -\infty, t) = 0, \qquad \phi(x = \infty, t) = 0, \quad t > 0, \qquad c(x, 0) = \exp\left(-\frac{(x - x_0)^2}{2\sigma_0^2}\right). \tag{30}$$

The exact solution is given by

$$c(x, t) = \frac{\sigma_0}{\sigma}\exp\left(-\frac{(x - \bar{x})^2}{2\sigma^2}\right), \tag{31}$$

in which

$$\sigma^2 = \sigma_0^2 + 2Dt, \qquad \bar{x} = x_0 + \int_0^t u(s)\mathrm{d}s. \tag{32}$$

We have used the following parameters in our simulations: $x_0 = 0$ and $\sigma_0 = 0{\cdot}1$. The numerical solutions are obtained at time $t = 0{\cdot}5$. As in the first example, we examine two transport modes: one is marginally advection–dominant transport with $Pe = 2$ and the other is strongly advection-dominant transport with $Pe = 50$. Both cases are simulated with $Cr = 0{\cdot}2$ and 1. The numerical solutions using a time weighting value $\alpha = 2$ are presented along with the analytical solution in Figure 5 for the case with $Pe = 2$. As observed in the previous example, the numerical solutions are virtually the same irrespective of the value of Courant number employed. For the strongly advection-dominant transport ($Pe = 50$) the numerical solutions using three selected time discretizations ($\alpha = 0{\cdot}5$, 1·75 and 2) are presented in Table III for $Cr = 0{\cdot}2$ and 1 in terms of the accuracy assessment parameters e_l, e_p and e_n defined earlier. Only the numerical solutions with $\alpha = 0{\cdot}5$ are presented along with the analytic solution in Figure 6. The numerical solutions with $\alpha = 0{\cdot}5$ are slightly better than those with $\alpha = 2$. The results of Figure 6 show good agreement between the exact and GEM solutions.

Using the second example with $D = 5 \times 10^{-4}$, the ability of the model to handle a situation where the velocity is time-dependent is examined. The imposed ambient velocity is given by

$$U(t) = 4\sin(4\pi t). \tag{33}$$

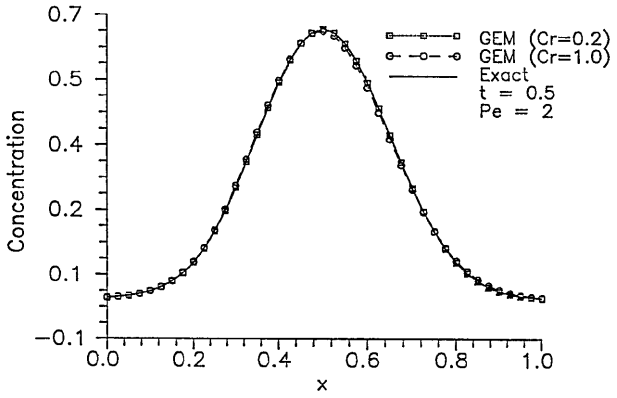

Figure 5. GEM and exact solution of example 2 with constant velocity ($Pe = 2$, $Cr = 0{\cdot}2$ and 1

A uniform time step of 5×10^{-3} is employed in the numerical calculations. The numerical and exact solutions at $t = 0{\cdot}5$ are presented in Figure 7, which shows good agreement of results.

The third example of transient 1D transport employed to validate our model is one in which first-order decay of the advecting containment is allowed to take place. The physical interpretation of this transport example, which brings out its engineering significance, is that of a contaminated stream being cleaned or decontaminated using mechanical means of advection from a freshwater source and a biological/chemical process which induces first-order decay of the pollutant. The initial and boundary conditions are

$$c(x, t = 0) = 1, \qquad c(x = 0, t > 0) = 0, \qquad \frac{\partial c(x = \infty, t > 0)}{\partial x} = 0. \tag{34}$$

The exact solution is[2]

$$c(x, t) = \exp(-\mu t)\left[1 - \frac{1}{2}\operatorname{erfc}\left(\frac{x - Ut}{2\sqrt{(Dt)}}\right) - \frac{1}{2}\exp\left(\frac{Ux}{D}\right)\operatorname{erfc}\left(\frac{x + Ut}{2\sqrt{(Dt)}}\right)\right], \tag{35}$$

where 'erfc' is the complementary error function. Two cases of this example with the following parameters are examined: (i) $U = 1, D = 0{\cdot}025$ with corresponding local Peclet $Pe = 2$ and $\mu = 0{\cdot}2$; (ii) $U = 1, D = 5 \times 10^{-4}$ with corresponding local Peclet $Pe = 50$ and $\mu = 0{\cdot}2$. The numerical calculations are done using a time weighting factor $\alpha = 2$ and a uniform spatial element size of 0·025, while $Cr = 1$ is used for case (i) and $Cr = 0{\cdot}2$ for case (ii). The numerical and exact solutions obtained at times $t = 0{\cdot}5$ and 1 are presented in Figure 8(a) for case (i) and in Figure 8(b) for case (ii). For case (i), which corresponds to mildly advection-dominant transport ($Pe = 2$), the exact solution is

Table III. Accuracy assessment values of numerical solutions with various time discretization schemes for example 2 ($Pe = 50$)

	$Cr = 0{\cdot}2$			$Cr = 1$		
α	e_l ($\times 10^{-3}$)	e_p ($\times 10^{-3}$)	e_n ($\times 10^{-5}$)	e_l ($\times 10^{-3}$)	e_p ($\times 10^{-3}$)	e_n ($\times 10^{-5}$)
0·5	5·56	1·28	2·98	85·83	3·12	1·06
1·75	41·89	17·46	1·02	230·10	91·40	0·31
2	7·28	1·01	3·48	110·90	29·49	1·81

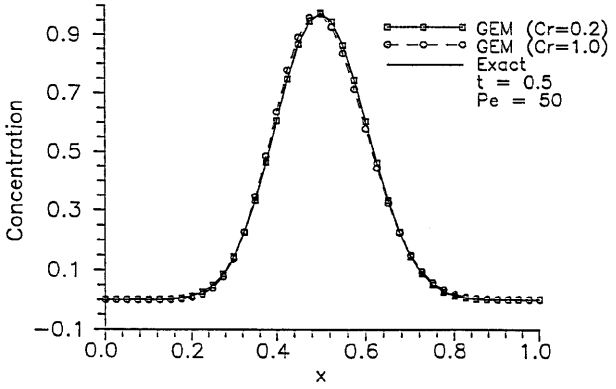

Figure 6. GEM and exact solution of example 2 with constant velocity ($Pe = 50$, $Cr = 0{\cdot}2$ and 1

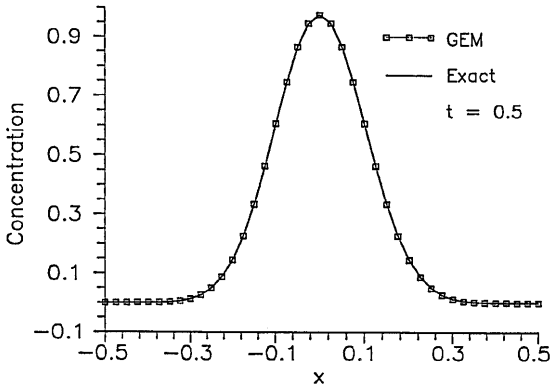

Figure 7. GEM and exact solutions of example 2 with time-dependent velocity for $Pe = 50$

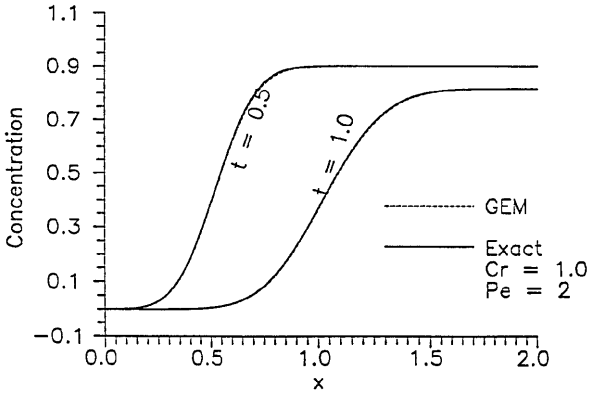

Figure 8(a). GEM and exact solutions of example 3 with first-order decay ($\mu = 0{\cdot}2$, $Pe = 2$ and $Cr = 1$

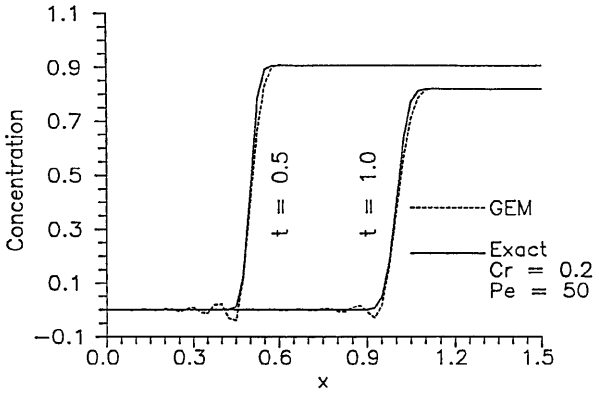

Figure 8(b). GEM and exact solutions of example 3 with first-order decay ($\mu = 0{\cdot}2$, $Pe = 50$ and $Cr = 0{\cdot}2$)

reproduced by the numerical scheme, while for case (ii), which corresponds to strongly advection-dominant transport ($Pe = 50$), the sharp front is reproduced by the numerical scheme but the numerical solution has trailing oscillations whose strength appears to be decreasing as the simulation time increases.

It should be noted that the applicability of the GEM has only been tested on analytical or closed-form solutions. Comparison with other methods was purposely avoided because it is not our intention at this stage to engage in a rather futile argument of claiming the superiority of one numerical method over another. It is our belief that most numerical methods in existence have their strong and weak points; the user can only be guided as to which method to adopt by a thorough understanding of the physics of the problem.

4. CONCLUSIONS

A new set of discrete element equations has been obtained for the transient 1D diffusion–advection equation with first-order decay for uniform or non-uniform flow velocity by a mixed Green element formulation. Using linear spatial elements and the free space Green function of the second-order derivative term, the formulation, based on the singular boundary element theory, discretizes the flow domain and incorporates a time-marching scheme in a typical finite element fashion. In contrasts, earlier attempts to adopt this combination have always taken the form of implementing the FEM in the problem domain and the BEM on the boundaries.[27–29] One advantage of our formulation is that the GEM adopts a finite element domain discretization that results in a banded global coefficient matrix which is easier to handle numerically. Because the formulation ensures C^0 continuity of the concentration and its first spatial derivative at the nodes and since the elemental integrals are evaluated in an exact manner, the discrete element equations exhibit stable characteristics even when advection is dominant. The three examples of transport problems examined show that incorporating the second-order-correct Crank–Nicolson scheme and the modified fully implicit scheme with a time weighting value of two produces the most superior solutions. For small values of local Peclet number or mildly advection-dominant transport, large time steps or large values of Courant number can be adopted to achieve acceptably good solutions, but for strongly advection-dominant transport or large values of local Peclet number, small time steps or small values of Courant number are required to achieve acceptable results. Further work is currently in progress to derive a theoretical analysis of the stability of this scheme.

REFERENCES

1. R. W. Clearly and M. J. Ungs, 'Analytical models for groundwater pollution and hydrology', *Rep. 78-WR-15*, Water Resources Program, Princeton University, 1978.
2. M. Th. van Genuchten and W. J. Alves, 'Analytical solutions of the one-dimensional convective–dispersive solute transportk equation', *Tech. Bull. 1661*, U.S. Department of Agriculture, 1982.
3. D. W. Peaceman and H. H. Rachford Jr., 'Numerical calculation of multi-dimensional miscible displacement', *Soc. Petrol. Eng. J.*, **2**, 327–339 (1962).
4. H. S. Price, J. C. Cavendish and R. S. Varga, 'Numerical methods of higher-order accuracy for diffusion–convection equations', *Soc. Petrol Eng. J.*, **16**, 293–300 (1968).
5. M. P. Anderson, 'Using models to simulate the movement of contaminant through groundwater flow systems', *CRC Crit. Rev. Environ. Control*, **9** 97–156 (1979).
6. O. C. Zienkiewicz and R. L. Taylor, *The Finite Element Method*, Vol. 2, McGraw-Hill, New York, 1991, Chap. 12, pp. 438–505.
7. W. G. Gray and G. F. Pinder, 'An analysis of the numerical solution of the transport equation', *Water Resources Res.*, **12** 547–555 (1976).
8. D. B. Spalding, 'A novel finite difference formulation for differential equations involving both first and second derivatives', *Int. j. numer. methods eng.*, **4**, 551–559 (1972).
9. J. C. Heinrich, P. S. Huyakorn, O. C. Zienkiewicz and A. R. Mitchell, 'An ''upward'' finite element scheme for two-dimensional convective transport equation', *Int. j. numer. methods eng.*, **11**, 131–143 (1977).
10. N.-Z. Sun and W. W.-G. Yeh, 'A proposed upstream weight numerical method for simulating pollutant transport in groundwater', *Water Resources Res.*, **19**, 1489–1500 (1983).
11. A. N. Brooks and T. J. R. Hughes, 'Streamline upwind/Petrov–Galerkin formulation for convection dominated flows with particular emphasis on incompressible Navier Stokes equation', *Comput. Methods Appl. Mech. Eng.*, **32**, 199–259 (1982).
12. E. Dick, 'Accurate Petrov–Galerkin methods for transient convective diffusion problems', *Int. j. numer. methods eng.*, **19**, 1425–1433 (1983).
13. C.-J. Chen and H.-C. Chen, 'The finite analytic method', *IIHR Rep. 232-IV*, University of Iowa, 1982.
14. O. O. Onyejekwe, 'A node-moving method of solution with application to the convection–diffusion equation', *Proc. 30th Heat Transfer and Fluid Mechanics Conf.*, Sacramento, CA, May 1987, pp. 81–87.
15. C. A. Brebbia and P. Skerget, 'Diffusion–advection problems using boundary elements', *Proc. 5th Int. Conf. on Finite Elements in Water Resources*, Burlington, VT, Springer-Verlag, 1984, pp. 747–768.
16. A. E. Taigbenu, 'A new boundary element formulation applied to unsteady aquifer problems', *Ph.D. Thesis*, Cornell University, 1985.
17. A. E. Taigbenu and J. A. Liggett, 'An integral solution for the diffusion–advection equation', *Water Resources Res.*, **22**, 1237–1246 (1986).
18. M. A. Aral and Y. Tang, 'A boundary-only procedure for transient transport problems with or without first-order chemical reaction', *Appl. Math. Model.*, **13**, 130–137 (1989).
19. A. E. Taigbenu, 'A more efficient implementation of the boundary element theory', *Proc. 5th Int. Conf. on Boundary Element Technology (BETECH 90)*, Newark, DE, 1990, pp. 355–366.
20. A. E. Taigbenu, 'The use of a higher interpolating function in conjunction with the Green element method', *Proc. Conf. on Computer Methods and Water Resources*, Rabat, October 1991, pp. 293–305.
21. A. E. Taigbenu and E. Sada, 'A Green element model for variably saturated groundwater flow', *Proc. Int. Conf. on Computational Methods in Water Resources*, Denver, CO, June 1992, Vol. 1, pp. 219–227.
22. A. E. Taigbenu, 'The Green element method', *Int. j. numer. methods eng.*, **38**, 2241–2263 (1995).
23. A. E. Taigbenu and O. O. Onyejekwe, 'Green element simulations of the transient nonlinear unsaturated flow equation', *Appl. Math. Model.*, **19**, 675–684 (1995).
24. A. E. Taigbenu and O. O. Onyejekwe, 'A mixed Green element formulation for transient Burgers equation', *Int. j. numer. methods fluids*, **24**, 563–578 (1997).
25. O. O. Onyejekwe, 'Green element description of mass transfer in reacting systems', *Numer. Heat Transfer*, B**30**, 483–498 (1996).
26. A. Ogata and R. B. Banks, 'A solution of the differential equation of longitudinal dispersion in porous media', *U.S. Geol. Surv. Prof. Paper 411-A*, 1961.
27. D. Ellsworth, 'A boundary element–finite procedure for porous and fractured media flow', *Water Resources Res.*, **12**, 551–560 (1987).
28. O. C. Zienkiewicz, D. W. Kelly and P. Bettes, 'The coupling of the finite element method and boundary solution procedures', *Int. j. numer methods eng.*, **11**, 355–375 (1977).
29. T. Krishnamurthy and I. S. Raju, 'Coupling finite element and boundary element methods for two-dimensional problems', *Int. j. numer. methods eng.*, **36**, 3395–3616 (1993).

